Neurobiology of Aging 57 (2017) 18–27

Contents lists available at ScienceDirect

Neurobiology of Aging

journal homepage: www.elsevier.com/locate/neuaging

# Prefrontal-parietal effective connectivity during working memory in older adults

Stephan Heinzel [a,b,c,*], Robert C. Lorenz [d,e], Quynh-Lam Duong [d], Michael A. Rapp [b,f], Lorenz Deserno [g,h]

[a] Department of Psychology, Freie Universität Berlin, Habelschwerdter Allee 45, Berlin 14195, Germany
[b] Social and Preventive Medicine, University of Potsdam, Am Neuen Palais 10, Potsdam 14469, Germany
[c] Department of Psychology, Humboldt-Universität zu Berlin, Rudower Chaussee 18, Berlin 12489, Germany
[d] Department of Psychiatry and Psychotherapy, Campus Charité Mitte, Charité, Universitätsmedizin Berlin, Charitéplatz 1, Berlin 10117, Germany
[e] Max Planck Institute for Human Development, Lentzeallee 94, Berlin 14195, Germany
[f] Cluster of Excellence NeuroCure, Charité-Universitätsmedizin Berlin, Germany
[g] Max Planck Institute for Human Cognitive and Brain Sciences, Stephanstraße 1A, Leipzig Germany
[h] Department of Child and Adolescent Psychiatry, Psychotherapy and Psychosomatics, University of Leipzig, Leipzig 04103, Germany

ARTICLE INFO

*Article history:*
Received 29 August 2016
Received in revised form 24 March 2017
Accepted 2 May 2017
Available online 10 May 2017

*Keywords:*
Aging
Dynamic causal modeling (DCM)
Effective connectivity
Functional magnetic resonance imaging (fMRI)
Working memory

ABSTRACT

Theoretical models and preceding studies have described age-related alterations in neuronal activation of frontoparietal regions in a working memory (WM) load-dependent manner. However, to date, underlying neuronal mechanisms of these WM load-dependent activation changes in aging remain poorly understood. The aim of this study was to investigate these mechanisms in terms of effective connectivity by application of dynamic causal modeling with Bayesian Model Selection. Eighteen healthy younger (age: 20–32 years) and 32 older (60–75 years) participants performed an n-back task with 3 WM load levels during functional magnetic resonance imaging (fMRI). Behavioral and conventional fMRI results replicated age group by WM load interactions. Importantly, the analysis of effective connectivity derived from dynamic causal modeling, indicated an age- and performance-related reduction in WM load-dependent modulation of connectivity from dorsolateral prefrontal cortex to inferior parietal lobule. This finding provides evidence for the proposal that age-related WM decline manifests as deficient WM load-dependent modulation of neuronal top-down control and can integrate implications from theoretical models and previous studies of functional changes in the aging brain.



## 1. Introduction

Aging is associated with a decline in working memory (WM) as indicated by a large number of studies comparing WM performance between younger and older adults (for reviews, see Craik and Salthouse, 2011; Verhaeghen and Cerella, 2002). In tasks including different levels of WM load, age-related performance decrements were found to be most apparent at high WM load (e.g., Nagel et al., 2011; Nyberg et al., 2009; Schneider-Garces et al., 2010). For several years, WM performance in older adults has been studied during functional neuroimaging, in particular using functional magnetic resonance imaging (fMRI), to examine neural correlates of the age-related decline in WM. Several earlier studies have reported pronounced activation mainly in frontoparietal areas during verbal WM tasks in older adults compared to younger adults (Cabeza et al., 2004; Logan et al., 2002; Reuter-Lorenz et al., 2000). However, when reviewing the literature, both hyper- and hypoactivations in frontoparietal regions including dorsolateral prefrontal cortex (DLPFC), lateral premotor cortex (LPMC), and inferior parietal lobule were detected during WM in older participants compared to their younger counterparts (Rajah and D'Esposito, 2005). It has been suggested that part of these conflicting results could be integrated by taking WM load into account; thus, hyperactivations were mainly found at relatively low WM load, whereas hypoactivations were most frequently reported at high WM load (Heinzel et al., 2014a; Nagel et al., 2011; Schneider-Garces et al., 2010). To replicate such previous findings and to confirm prior region of interest (ROI)-based analyses from a subsample of the present study (Heinzel et al., 2014a), we performed fMRI whole-brain analyses in an extended sample.

The "Compensation-Related Utilization of Neural Circuits Hypothesis" (CRUNCH) by Reuter-Lorenz and Cappell (2008) describes age-related hyperactivations at low WM load in terms of

* Corresponding author at: Department of Psychology, Freie Universität Berlin, Habelschwerdter Allee 45, Berlin 14195, Germany. Tel.: +49(0)30838 61564; fax: +49(0)30838 461564.
*E-mail address:* stephan.heinzel@fu-berlin.de (S. Heinzel).

0197-4580/$ – see front matter © 2017 Elsevier Inc. All rights reserved.
http://dx.doi.org/10.1016/j.neurobiolaging.2017.05.005

reduced neural efficiency and hypoactivations at high WM load in terms of reduced neural capacity (Barulli and Stern, 2013). In a more general framework (the "Scaffolding Theory of Aging and Cognition", this pattern of both reduced neural efficiency and capacity has been described as reduced neural "adaptivity" (Park and Reuter-Lorenz, 2009; Reuter-Lorenz and Park, 2014). In the context of WM, this resembles the notion that younger adults are able to adapt task-related activity according to increasing WM load, whereas older adults require compensational activation already at low WM load and are unable to further recruit neural resources at high WM load. In line with previous n-back research (e.g., Nagel et al., 2011; Nyberg et al., 2009), "low WM load" refers to 1-back, whereas "high WM load" refers to 3-back in the present study. When testing interindividual differences within older participants, previous research (for review see Grady, 2012; Nyberg et al., 2012; Stern et al., 2005) suggests that participants with less performance decrements in challenging cognitive tasks may also show more "youth-like" (Nagel et al., 2011) brain activation patterns. Better WM performance was associated with higher WM load-dependent adaptivity of neural activations (i.e., low activation at low WM load [1-back] and high activation at high WM load [3-back], Nagel et al., 2011; Nyberg et al., 2009). Although this concept of adaptivity has been operationalized and investigated predominantly in terms of neural activity, underlying network dynamics that may govern these neural activities remain largely unknown. Recently, a few studies have tested correlation-based functional connectivity in older age, indicating deficient frontoparietal coupling that may relate to changes in neural activity (Heinzel et al., 2014a; Matthäus et al., 2012; Nagel et al., 2011; Steffener et al., 2012). It has been suggested that these alterations might be due to an age-related deficit in prefrontal top-down control over posterior regions (Gazzaley et al., 2005; Gazzaley and D'Esposito, 2007).

However, no models of effective connectivity, such as dynamic causal modeling (DCM, Friston et al., 2003), supporting this proposal have been tested in older adults to date. In younger adults, increasing WM load-dependent effective connectivity from DLPFC to IPL ("top-down"/"backward") best explained fMRI data acquired during a numeric "n-back" WM task (Deserno et al., 2012). Until now, it has not been investigated how aging may alter this architecture of WM load-dependent prefrontal to parietal effective connectivity. Thus, the aim of the present study was to go beyond correlational connectivity approaches and to test competing directional neuronal models of WM-dependent frontoparietal effective connectivity in older age for the first time. Results could improve the understanding of underlying mechanisms in terms of network dynamics of age-related WM deficits and integrate notions from compensation and top-down control models of aging. Therefore, we applied DCM (Friston et al., 2003) complemented by Bayesian model selection (BMS) techniques (Stephan et al., 2009) to fMRI data of younger and older adults performing a numeric n-back WM task as used in previous studies (Deserno et al., 2012; Heinzel et al., 2014a; Owen et al., 2005).

According to previous work (Nee et al., 2013; Owen et al., 2005), 3 nodes were identified to represent a simplified model of frontoparietal top-down control during WM: DLPFC, LPMC, and IPL. During WM, IPL was found to be involved in processes of information storage (Chein and Fiez, 2010; Christophel et al., 2012; Guerin and Miller, 2011; Todd and Marois, 2004), and DLPFC has been suggested to play a key role in top-down control of WM storage (Curtis and D'Esposito, 2003; Edin et al., 2009) potentially by guiding the selection of relevant and suppression of irrelevant information (Gazzaley et al., 2007; McNab and Klingberg, 2008; Montojo and Courtney, 2008). The LPMC has been associated with the attention-based rehearsal in WM (Baddeley, 2003; Bledowski et al., 2010; Curtis and D'Esposito, 2003) and was found to be most strongly involved at high task demands during WM updating (Nee et al., 2013; Wager and Smith, 2003).

In the present study, the following hypotheses were tested:

1. Older adults show lower WM performance, specifically at high WM load.
2. Older adults show increased neural activation at low (1-back) and decreased activation at high (3-back) WM load in frontoparietal WM regions, indicating reduced WM load-dependent adaptivity of neural activations.
3. FMRI data are best explained by a "backward" model, comprising a modulatory connection from DLPFC to IPL, supporting notions from "top-down" control models.
4. Older adults show a reduced WM load-dependent modulation of DLPFC to IPL connectivity, thus proposing an extension of the concept of WM load-dependent adaptivity in terms of effective connectivity.
5. High-performing older adults show higher WM load-dependent modulation of DLPFC to IPL connectivity compared to low-performing older adults.

## 2. Methods

### 2.1. Participants and screening instruments

Thirty-four older participants (age: 60–75 years) and 18 younger participants (age: 21–30 years) were recruited via newspaper and online announcements in Berlin, Germany. All participants were native German speakers, right-handed, had normal or corrected-to-normal vision, no history of any neurological or psychiatric diseases, and did not take any psychiatric medication. Mini-Mental Status Examination (Folstein et al., 1975) was 27 or above in all participants. All participants were suitable for fMRI, and none of the participants took any antihypertensive medication or had a thyroidal dysfunction, which could have influenced the blood-oxygen-level-dependent (BOLD) signal. In the older group, 1 participant had to be excluded from analyses due to a technical failure during the fMRI scanning, and another participant had to be excluded due to model nonconvergence. Therefore, the final sample consisted of 32 participants (23 women) in the older group (mean age = 65.25 [± 3.81] years) and 18 participants (10 women) in the younger group (mean age = 24.06 [± 2.41] years). The groups did not differ significantly in gender distribution, education level, verbal intelligence (measured by a German vocabulary test [Schmidt and Metzler, 1992]), and Mini-Mental Status Examination (all $P$'s $> 0.22$). Further demographic information is reported in Table 1. The study was approved by the ethics committee of the Charité–Universitätsmedizin, Berlin. Written informed consent was obtained from all participants prior to investigation. Participants who completed the study received a monetary reimbursement.

### 2.2. n-back WM task

In this study, a computerized version of the n-back paradigm with numerical stimuli was adapted from previously used n-back paradigms (Cohen et al., 1997; Heinzel et al., 2014b,c). The n-back task was programmed using Presentation software (version 14.9; Neurobehavioral Systems Inc, Albany, CA, USA). The n-back task consisted of 2 sessions. In each session, 16 blocks were presented in 4 different pseudorandomized orders counterbalanced across participants. The total duration of the task was 22 minutes. WM load (0-, 1-, 2-, and 3-back) was varied between blocks. Please note that in the n-back task, as used in the present study, the term 'WM load' refers to the amount of stimuli that need to be processed

**Table 1**
Demographics (means ± standard deviations)

| Variable | Younger (N = 18) | Older (N = 32) | Younger versus older t(48) [*p*-value] |
|---|---|---|---|
| Age | 24.06 [± 2.41] | 65.25 [± 3.81] | 41.35 [<0.001] |
| Sex | 8m/10f | 9m/23f | Chi square (50,1) = 1.37, $p = 0.352$ |
| Education (years) | 16.36 [± 1.86] | 15.50 [± 3.36] | 1.00 [0.321] |
| Verbal intelligence (WST) | 33.83 [± 3.88] | 33.72 [± 2.49] | 0.13 [0.899] |
| Mini-mental status examination | 29.50 [± 0.79] | 29.16 [± 1.02] | 1.24 [0.222] |
| 0-back performance | 0.99 [± 0.02] | 0.98 [± 0.03] | 1.55 [0.129] |
| 1-back performance | 0.95 [± 0.04] | 0.90 [± 0.09] | 2.43 [0.019] |
| 2-back performance | 0.78 [± 0.10] | 0.63 [± 0.12] | 4.42 [< 0.001] |
| 3-back performance | 0.58 [± 0.09] | 0.43 [± 0.13] | 4.22 [< 0.001] |
| RT 0-back | 399 [± 31] | 445 [± 63] | 2.94 [= 0.005] |
| RT 1-back | 462 [± 62] | 535 [± 83] | 3.28 [= 0.002] |
| RT 2-back | 556 [± 81] | 653 [± 100] | 3.51 [= 0.001] |
| RT 3-back | 669 [± 128] | 735 [± 108] | 1.94 [= 0.058] |

WST, vocabulary test.

simultaneously to accomplish the task and does not imply that an increasing n-back load involves the same processes at all load levels. The WM load condition of each block was indicated by a cue 2 seconds before the block started. In each block, 16 randomly created digits from 0 to 9 were presented in the center of a black screen one at a time for 500 ms with an interstimulus interval of 500 or 1500 ms (pseudorandomized across blocks); the occurrence of 5 target stimuli was pseudorandomized. Targets were defined as reoccurrence of a number previously presented 1, 2, or 3 trials before (1-, 2-, or 3-back condition). In the 0-back condition, the target was defined as the number '0'. The participants were instructed to press a button with their right thumb when they recognized a target. After each block, a white fixation cross was presented in the center of a black screen for 12 seconds. For statistical analysis, Kolmogorov-Smirnov test was applied to test for deviations from a normal distribution. As 0-back performance was found to be not normally distributed, it was not included in the age group (older vs. younger) by WM load (1-, vs. 2-, vs. 3-back) analysis of variance (ANOVA.)

### 2.3. MR image acquisition

FMRI data were collected at 2 study centers. Twenty-six participants (19 in older and 7 in the younger group) were scanned at Charité Virchow Campus, Berlin with a 3 Tesla GE Signa Excite (General Electrics Medical Systems, Milwaukee, USA) and 24 participants (13 in the older and 11 in the younger group) at Charité Campus Mitte, Berlin with a 3 Tesla Magnetom Trio Tim MR system (Siemens, Erlangen, Germany). Chi-square tests indicated no significant differences in distribution of groups and sex across scanner sites (all *P*'s > 0.23). At the beginning of each scanning procedure, 1 T1-weighted 3D pulse sequence was obtained (repetition time [TR] = 7.8 ms, echo time [TE] = 3.164 ms, flip angle = 20°, field of view [FoV] = 256 × 256 $mm^2$, matrix size = 256 × 256, 176 sagittal slices with 1-mm thickness, voxel size = 1 × 1 × 1 $mm^3$). Functional data were assessed using a gradient-echo echo-planar imaging (GE-EPI) pulse sequence (TR= 2000 ms, $TE_{GE}$ = 35 ms, $TE_{Trio}$ = 32 ms, flip angle = 80°, matrix size = 64 × 64, voxel size = 3.1 × 3.1 × 3.8 mm). 31 slices were acquired approximately axial to the bicommissural plane. To take into account that participants were tested at 2 different scanner sites, scanner site was included as a covariate in behavioral and fMRI analyses.

### 2.4. MR image processing and analysis

#### 2.4.1. Preprocessing

All fMRI analyses were carried out with SPM8 (Wellcome Department of Imaging Neuroscience, London, UK). After correction for head motion and computation of a mean EPI image, the high-resolution T1-weighted anatomical image of each participant was coregistered to their mean EPI image and was normalized by applying the unified segmentation technique (Ashburner and Friston, 2005). EPIs were resampled into isotropic voxels with an edge length of 3.3 mm and spatially smoothed with an isotropic Gaussian kernel of 8 mm full width at half maximum. No slice time correction was applied.

#### 2.4.2. Estimation of BOLD effect sizes

The block design n-back WM experiment was analyzed within the framework of the General Linear Model (GLM). Hemodynamic responses were modeled using the canonical hemodynamic response function as contained in SPM at onsets of each block for the duration of each block (16 or 32 seconds). At the single-subject level, experimental conditions of 0-, 1-, 2-, and 3-back were included as separate regressors of interest and all other events (cue, button presses) as well as the 6 rigid body realignment parameters as regressors of no interest. The GLM was fitted voxel-wise to the filtered time series using the restricted maximum likelihood algorithm as implemented in SPM8. To measure WM-related activation, differential contrasts of 1-back versus 0-back, 2-back versus 0-back, and 3-back versus 0-back were computed. On the group level, a 2 (age group) by 3 (WM load) ANOVA with the covariate scanner site was computed within the whole brain (no masking was applied). Please note, a subsample has previously been reported in a ROI-based analysis (Heinzel et al., 2014a) and an analysis of training and transfer effects (Heinzel et al., 2016). For SPM analyses on the group level, family-wise error correction on the voxel level ($p < 0.05$, corrected for the whole brain) was applied. To test overlap between results from the whole-brain analysis and literature-based ROIs used for data extraction in the DCM analyses, we built 1 combined ROI from the 6 literature-based probabilistic ROIs (bilateral DLPFC, IPL, and LPMC) and additionally used this for post hoc small-volume correction ($p < 0.05$ family-wise error corrected [FWE-corr] for small volume).

### 2.5. Dynamic causal modeling

DCM10 for fMRI as implemented in SPM8 update revision 5236 was used. The focus of DCM for fMRI is the analysis of a priori selected regional time series to analyze effective connectivity and its modulation by experimental perturbations. This is addressed by modeling the hidden internal and external neuronal dynamics within the selected network of regions of interest (Friston et al., 2003). Here, we applied bilinear, deterministic DCM with mean-centered inputs. Thus, parameters of such a DCM describe the endogenous (average) coupling between 2 regions, which is context

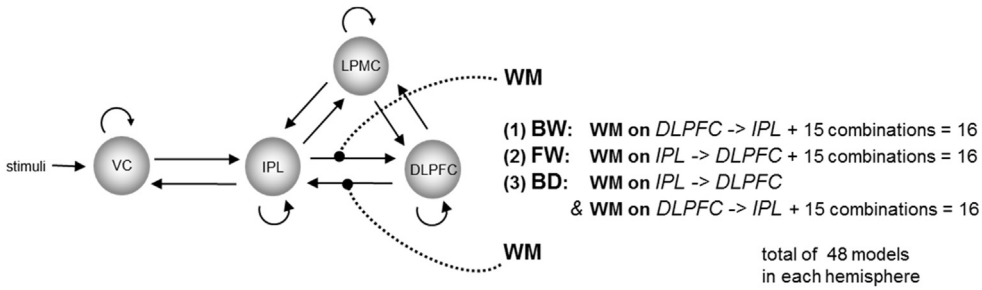


**Fig. 1.** Model space. Models: BW, backward; FW, forward; BD, bidirectional. Abbreviations: DLPFC, dorsolateral prefrontal cortex; IPL, intraparietal lobule; LPMC, lateral premotor cortex; VC, visual cortex; WM, working memory.

independent ("intrinsic connections") and also the impact of experimental stimuli that can be modeled directly on specific regions ("driving inputs") or on the strength of coupling between 2 regions ("modulatory input"). By application of a hemodynamic forward model (Friston et al., 2000; Stephan et al., 2009), the modeled neuronal dynamics of the system are transformed into a measured response, in the present study the BOLD signal. Parameter estimation is performed in a fully Bayesian framework as described previously in detail (Friston et al., 2003).

### 2.5.1. Region selection and time series extraction

Previous work (Deserno et al., 2012; Schmidt et al., 2013) and results of our GLM analysis motivated a focus on prefrontal-parietal connectivity. Therefore, DLPFC and IPL were included. As an extension of our previous study (Deserno et al., 2012), we added LPMC based on its robust activation during WM (Owen et al., 2005) and its potential role in focus shifting in rehearsal and response preparation (Bledowski et al., 2009; Rottschy et al., 2012). The visual cortex (VC) was added as a region for driving inputs as stimulation took place visually during the applied n-back task. Regional time series for DLPFC, IPL, and LPMC were extracted on the single-subject level based on ROIs that were derived from the literature providing frontoparietal coordinates during n-back performance. These ROIs (Fig. 3B) were created combining anatomical hypotheses with functional findings (spatial coordinates) as reported in 23 previous studies using verbal n-back tasks. The method of ROI computation was described in detail previously (Heinzel et al., 2014a) and is also reported in Supplementary Material. For VC, an ROI was computed by multiplying the group-level VC cluster for a contrast comprising all visual events (all n-back blocks and all instruction trials) versus implicit baseline (fixation cross) at p-FWE $< 0.05$ with an anatomical mask of Brodmann area (BA) 17 as obtained in the WFU Pick Atlas (Lancaster et al., 2000; Maldjian et al., 2003). For time series extraction, we first searched for each individual's MNI coordinates of maximum *t*-value within the ROIs for a contrast of interest: all WM conditions (3-, 2-, and 1-back) versus 0-back for DLPFC, IPL, and LPMC whereas the contrast comprising all visual events versus baseline was applied for VC. At each participant's peak coordinates surrounded with 4-mm spheres, the mean parameter estimates (adjusted for effects of interest) were extracted.

### 2.5.2. Model space

Constant across all models (Fig. 1), we assumed bidirectional, intrinsic connectivity between DLPFC, LPMC, and IPL, as well as bidirectional intrinsic connections between IPL and VC (A-matrix). All visual events were directed to VC as driving inputs. 3-, 2-, and 1-back conditions were included as contextual, WM-dependent modulation on frontoparietal connections. In previous work (Deserno et al., 2012), we demonstrated that a backward (BW)-modulation of WM on DLPFC to IPL connectivity explained the data of healthy participants best. Here, we aimed to replicate this finding in younger participants. Therefore, and in a first step, we constructed 3 initial models as in our previous study: (1) we assumed a BW-modulation of WM on DLPFC to IPL to be the main characteristic of the investigated network (Fig. 1). In addition, we implemented 2 alternative models with (2) a forward (FW)-modulation of WM on IPL to DLPFC or (3) a bidirectional (BD)-modulation as the main characteristic of the frontoparietal network (Fig. 1). In a second step, each of the 3 models were allowed to vary as a function of WM-dependent influences on the remaining connections between IPL and LPMC as well as DLPFC and LPMC by implementing all possible combinations. No modulatory influences were allowed on the connections between VC and IPL. Thus, we constructed 15 possible combinations of the modulatory input WM with the 4 intrinsic connections between IPL and LPMC as well as DLPFC and IPL. Each of the 3 initial models were combined with these 15 models. This resulted in 3 families of models (BW, FW, and BD) each containing 16 models, resulting in a total of 48 models tested. A description of all single models is also reported in Supplementary Material. These models were estimated separately within the right and the left hemisphere.

### 2.5.3. Bayesian model selection

To compare these 3 families of models and also search for single best fitting models in both groups, BMS was applied. In general, BMS takes into account the fit of a model, how well the parameters account for the data, and, in relation to the model complexity, the

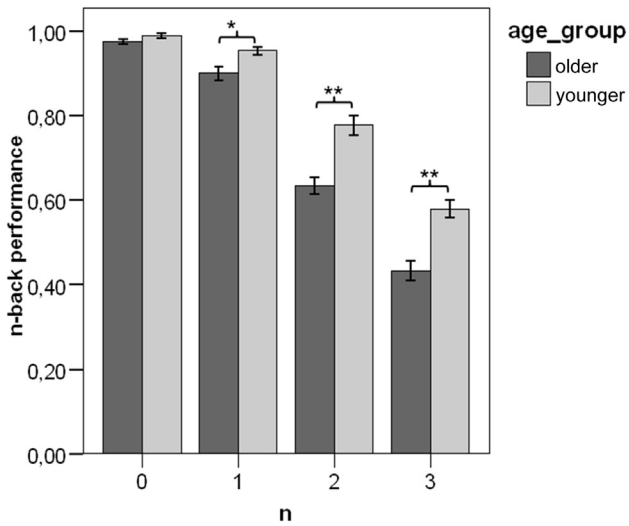


**Fig. 2.** Mean values and standard errors of mean of performance (hitrate minus false alarm rate) in the 4 working memory load conditions (0-, 1-, 2-, and 3-back) in younger and older participants. $^{*}p < 0.05$ and $^{**}p < 0.0125$ (Bonferroni corrected for 4 planned comparisons).

number of parameters. With higher complexity, the relative fit of a model may increase but generalizability may decrease. For BMS, we used a random-effects approach (Stephan et al., 2009). Random-effects BMS yields so-called exceedance probabilities, the probability that 1 model is more likely than another. BMS was first applied at the family level to compare the 3 families of models as previously described (Penny et al., 2010). Specifically, BMS was conducted for younger and older participants separately to test for different neuronal, WM-dependent architecture in the frontoparietal WM-network between groups.

## 3. Results

### 3.1. N-back performance in younger and older adults

To test whether differences between age groups in n-back performance (defined as hit rate minus false alarm rate) were related to WM load, a 2 (age group) by 3 (WM load) ANOVA with scanner site as covariate was conducted. A significant main effect of WM load ($F[2,94] = 112.31$, $p < 0.001$, partial $\eta^2 = 0.705$) showed that n-back performance decreased with higher load levels irrespectively of age. Younger participants outperformed older participants irrespectively of WM load, as demonstrated by a significant main effect of age group ($F[1,47] = 30.04$, $p < 0.001$, partial $\eta^2 = 0.390$). Most importantly, a significant 2-way interaction ($F[2,94] = 3.25$, $p = 0.043$, partial $\eta^2 = 0.065$) was revealed, indicating larger age differences in n-back performance with increasing WM load (Fig. 2). Post hoc ANOVAs using only 2 levels of WM load showed that age differences in WM performance increased from 1- to 2-back and from 1- to 3-back (both $p$'s $< 0.05$) but did not increase from 2- to 3-back ($p = 0.932$). Post hoc $t$ tests showed that n-back performance of younger adults was higher in 1-back ($T(48) = 2.43$, $p = 0.019$), 2-back ($T(48) = 4.42$, $p < 0.001$), and 3-back ($T(48) = 4.22$, $p < 0.001$). There was neither a main effect of scanner site nor an interaction between scanner site and WM load (all $p$'s $> 0.51$). Analyses of response time (RT) indicated a nonsignificant group by WM load interaction ($F(1,47) = 1.14$, $p = 0.325$, partial $\eta^2 = 0.024$). However, a significant main effect of age group ($F(1,47) = 8.54$,

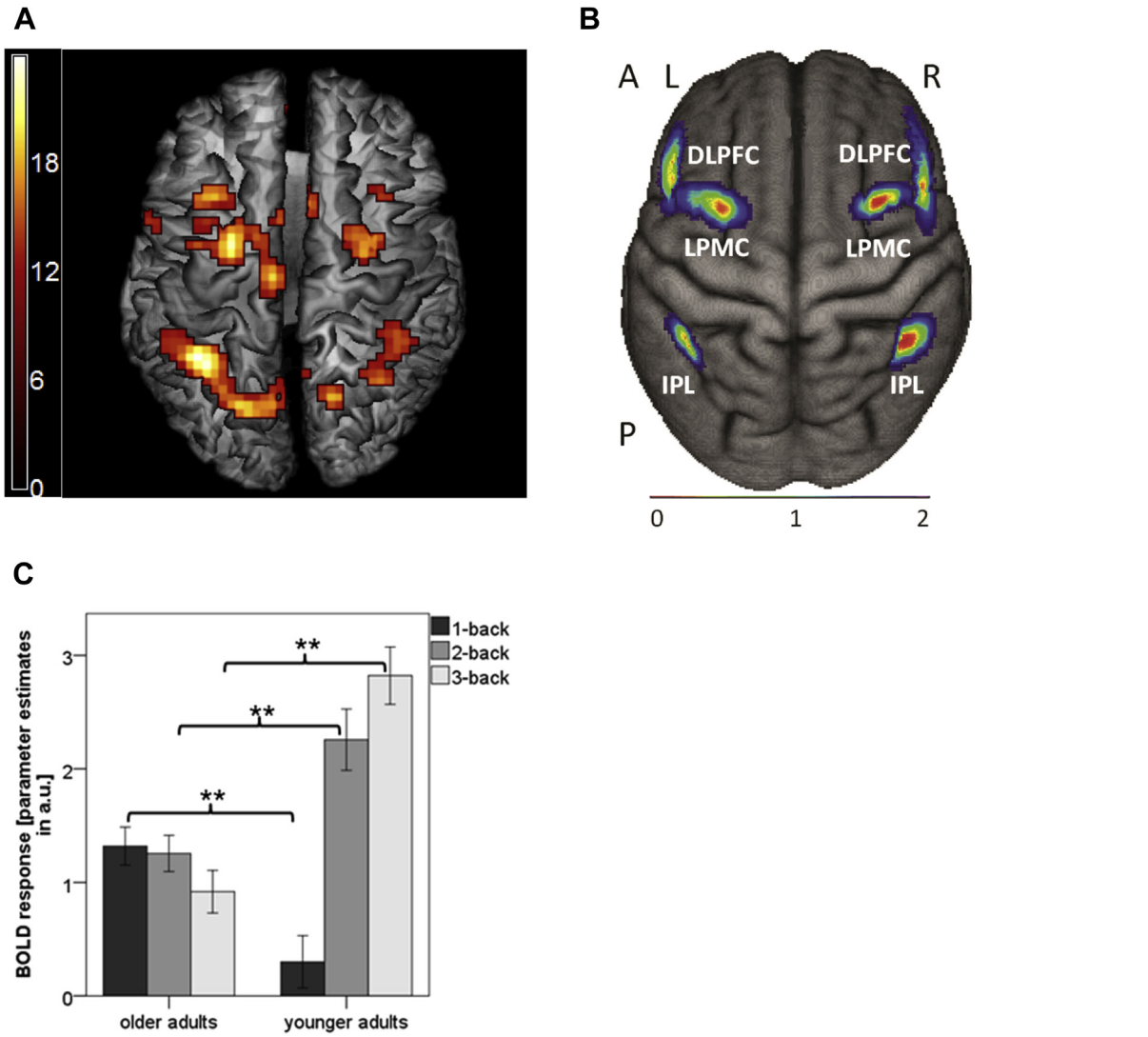


**Fig. 3.** (A) Results of the whole-brain analysis of age group by WM load are shown at significance threshold $p < 0.001$, uncorrected, k > 10 for display purposes; peak coordinates of all clusters that are significant at $p < 0.05$ FWE corrected for whole brain are reported in Table 2. (B) Probabilistic literature-based regions of interest (ROIs) include dorsolateral prefrontal cortex (DLPFC), lateral premotor cortex (LPMC), and inferior parietal lobule (IPL). The color code indicates the standard deviation (SD) from ROI center. (C) Means and standard errors of mean parameter estimates of significant voxels of the age group by WM load interaction ($p < 0.05$ FWE-corrected for whole brain) adjusted for effects of interest, in arbitrary units (a.u.). $^{**}p < 0.0167$ (Bonferroni corrected for 3 planned comparisons). Abbreviations: A, anterior; L, left hemisphere; P, posterior; R, right hemisphere.

**Table 2**
Anatomical locations and MNI coordinates for the WM load (1-back, 2-back, and 3-back) by age group (younger vs. older participants) interaction, whole-brain results reported at $p < 0.05$, family-wise error-corrected (FWE-corr), $k \geq 5$ voxels

| Region | Cluster Size | HEM | BA | MNI Coordinates | | | F-value | $p_{FWE\text{-}corr}$ |
|---|---|---|---|---|---|---|---|---|
| | | | | x | y | z | | |
| Inferior parietal lobule | 107 | L | 40 | −38 | −49 | 46 | 23.77 | <0.001 |
| Superior parietal lobule | | L | 7 | −22 | −69 | 49 | 19.31 | 0.001 |
| Precuneus | | L | 7 | −9 | −69 | 49 | 17.01 | 0.004 |
| Middle frontal gyrus | 47 | L | 6 | −25 | −3 | 52 | 22.39 | <0.001 |
| Thalamus | 16 | L | | −9 | −16 | 13 | 19.46 | 0.001 |
| Insula | 21 | L | 13 | −32 | 17 | 6 | 18.55 | 0.001 |
| Superior parietal lobule | 13 | R | 7 | 14 | −66 | 56 | 18.38 | 0.002 |
| Middle frontal gyrus | 40 | R | 6 | 28 | −6 | 49 | 17.63 | 0.003 |
| Middle frontal gyrus | | R | 6 | 31 | 0 | 56 | 17.04 | 0.004 |
| Cingulate gyrus/medial frontal gyrus | 26 | R | 32 | 4 | 13 | 46 | 17.47 | 0.003 |
| Cerebellum posterior lobe | 5 | R | | 34 | −59 | −30 | 16.30 | 0.007 |
| Thalamus | 6 | L | | −15 | 0 | 13 | 15.27 | 0.015 |
| Inferior parietal lobule | 8 | R | 40 | 41 | −39 | 36 | 14.91 | 0.019 |

Key: BA, Brodmann area; Hem, hemisphere; L, left; R, right.

$p = 0.005$, partial $\eta^2 = 0.154$) showed generally higher RTs in older compared to younger participants. The main effect for WM load ($F(2,94) = 88.77$, $p < 0.001$, partial $\eta^2 = 0.654$) indicated higher RTs with increasing WM load. Performance and RTs for all conditions are reported in Table 1.

### 3.2. fMRI GLM results

An age group by WM load full factorial ANOVA, including scanner site as a covariate, showed a significant interaction of age group by WM load that reached significance at $p<0.05$ FWE-corr at the whole brain in bilateral inferior parietal lobule, superior parietal lobule, middle frontal gyrus, and cingulate gyrus, as well as left precuneus, thalamus, and insula (Fig. 3, panel A). No significant interactions with the covariate scanner site were detected. In Table 2, we report whole-brain results of the interaction age group by WM load at $p < 0.05$ FWE-corr and a cluster threshold of $k \geq 5$ voxels. To indicate all task-active brain areas, we report the main effect of WM in the Supplementary Table S1 and in Supplementary Fig. S1. As depicted in Fig. 3, panel C, the WM load by group interaction indicates relatively higher activations at 1-back ($T(48) = 3.61$, $p = 0.001$) and lower activation at 2- ($T(48) = 3.41$, $p = 0.001$) and 3-back ($T(48) = 6.07$, $p < 0.001$) in the older compared to the younger group. As displayed in the Supplementary Fig. S2, similar activation patterns of the age group by WM interaction were found significant within each of the literature-based ROIs ($p < 0.05$ FWE-corrected for small-volume (the 6 ROIs combined in 1 ROI]) as used for time-series extraction for DCM analyses. This additional post hoc analysis ensures regional consistency between GLM results and the subsequent DCM results.

### 3.3. Effective connectivity: DCM

#### 3.3.1. Bayesian model selection

First, the 3 families of models partitioning modulatory influences of WM on frontoparietal connections ("backward" [BW], "forward" [FW], and "bidirectional" [BD]) were compared. BW models included a modulatory connection from DLPFC to IPL, FW models from IPL to DLPFC, and BD models from DLPFC to IPL and from IPL to DLPFC. In the entire sample, the BW family best explained the data in both hemispheres (exceedance probability in the left hemisphere 94.86% for BW, 5.13% for FW, and 0.01% for BD; in the right hemisphere 88.77% for BW, 11.23% FW, and 0.00% for BD). On the level of single models, model 1 (WM-modulated connectivity only from DLPFC to IPL) showed the highest exceedance probability in both hemispheres (left hemisphere: 31.34%, right hemisphere: 82.24%).

When comparing families of models in young and older participants separately, exceedance probabilities in young participants were, in left hemisphere: 72.86% for BW, 27.12% for FW, and 0.02% for BD; and in right hemisphere: 55.83% for BW, 43.55% for FW, and 0.62% for BD. Exceedance probabilities in older participants were, in left hemisphere: 93.52% for BW, 5.78% for FW, and 0.07% for BD; and in right hemisphere: 92.67% for BW, 7.33% for FW, and 0.00% for BD. Graphs of the family selection results are depicted in the Supplementary Fig. S2. BMS results regarding all single 48 models are listed in the Supplementary Table S2 as a function of hemisphere and age group. Taken together, results indicate that the data were explained best by a BW model family in both age groups, as suggested by previous work (Deserno et al., 2012). However, in the right hemisphere, higher model variability was found in younger adults.

#### 3.3.2. WM-dependent effective connectivity

Parameter estimates of effective connectivity from DLPFC to IPL, derived from the overall best fitting model (model 1), were compared in a hemisphere by WM load by age group ANOVA with scanner site as covariate (see Fig. 4 Panels A and B). A significant main effect of WM load ($F(1,47) = 40.75$, $p < 0.001$, partial $\eta^2 = 0.464$) showed that DLPFC to IPL connectivity increased with increasing WM load across both hemispheres and both age groups. A significant main effect of hemisphere ($F(1,47) = 4.39$, $p = 0.042$, partial $\eta^2 = 0.085$) indicated overall higher connectivity in left compared to right hemisphere. On a trend level, connectivity was overall higher in younger compared to older adults (main effect of group, $F(1,47) = 3.48$, $p = 0.069$, partial $\eta^2 = 0.069$). No significant hemisphere by WM load by age group interaction ($F(2,94) = 0.002$, $p = 0.998$, partial $\eta^2 = 0.000$) nor any other interaction effects including hemisphere as a factor were found (all $p$'s $> 0.37$). However, a significant WM load by age group interaction $F(2,94) = 24.78$, $p < 0.001$, partial $\eta^2 = 0.345$) indicated that WM load-dependent connectivity differs between younger and older adults in both hemispheres. This result was confirmed by exploratory post hoc WM load by age group ANOVAs in each hemisphere separately (left hemisphere: $F(2,94) = 22.14$, $p < 0.001$, partial $\eta^2 = 0.320$; right hemisphere: $F(2,94) = 15.90$, $p < 0.001$, partial $\eta^2 = 0.253$). Post hoc 2-sample $t$ tests showed that left hemispheric connectivity was higher in younger compared to older adults in 2-back ($T(48) = 2.89$, $p = 0.006$) and 3-back ($T(48) = 3.03$, $p = 0.004$), whereas no

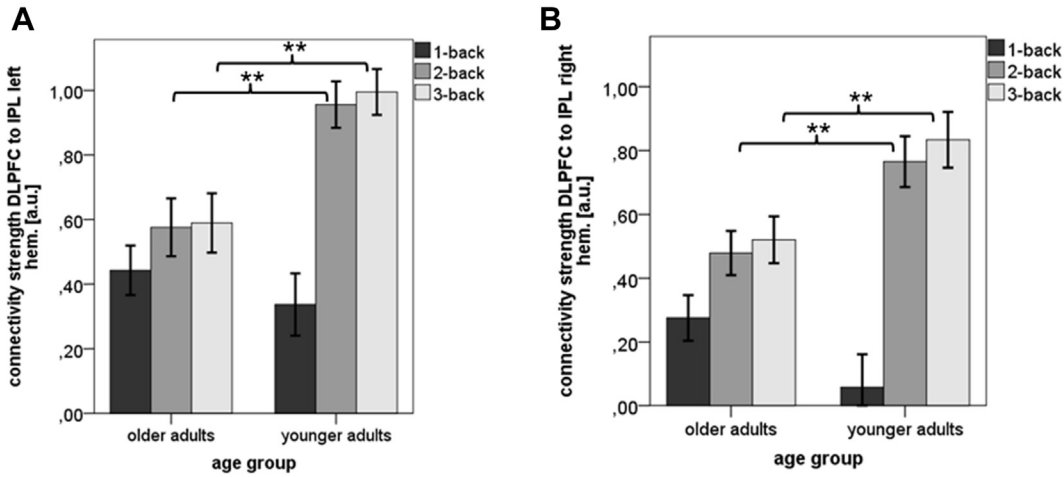


**Fig. 4.** Mean parameter estimates of effective connectivity ± standard error of the best fitting model (model 1) according to the Bayesian model selection (BMS) analysis. The DLPFC to IPL connectivity is displayed in older versus younger participants in the left (panel A) and right hemisphere (panel B). $^{**}p < 0.0167$ (Bonferroni corrected for 3 planned comparisons).

differences were found in 1-back ($T(48) = 0.85$, $p = 0.402$). In the right hemisphere, there was a trend for higher connectivity in older adults in 1-back ($T(48) = 1.77$, $p = 0.083$), while younger adults showed higher connectivity in 2-back ($T(48) = 2.60$, $p = 0.012$) and 3-back ($T(48) = 2.66$, $p = 0.011$). No main effect of scanner site $F(1,47) = 0.17$, $p = 0.685$, partial $\eta^2 = 0.004$) nor any interactions including scanner site as a factor were significant (all $p$'s $> 0.37$).

### 3.3.3. Behavior subgroup analyses in older adults

To further understand neuronal underpinnings of inter-individual differences regarding WM deficits in older adults, the older sample was divided in 2 subgroups according to their mean WM performance by a median split. As proof of concept, the high-performance group showed higher performance in 1-, 2-, and 3-back compared to the low-performance group ($p$'s $< 0.05$). A hemisphere by WM load by performance group ANOVA with scanner site as covariate was conducted on effective connectivity from DLPFC to IPL, a significant 3-way interaction was found ($F(2,58) = 4.03$, $p = 0.023$, partial $\eta^2 = 0.122$). As shown in Fig. 5, panel A, in the left hemisphere, no significant WM load by performance group interaction was found ($F(2,58) = 0.52$, $p = 0.598$, partial $\eta^2 = 0.018$), whereas in the right hemisphere (Fig. 5, panel B), this WM load by performance group interaction was significant ($F(2,58) = 3.91$, $p = 0.026$, partial $\eta^2 = 0.119$). Follow-up paired $t$ tests indicated that DLPFC to IPL connectivity increased significantly from 1-back to 2-back ($T(15) = 2.86$, $p = 0.012$) and from 1-back to 3-back ($T(15) = 4.43$, $p < 0.001$) in the high performance group but not in the low performance group of the older participants (all $p$'s $> 0.15$). Thus, the ability to adapt right hemispheric effective DLPFC to IPL connectivity to increasing WM load was related to higher performance in the older sample, whereas the inability to further increase this connectivity was found to be associated with lower performance. This WM load-dependent pattern was not revealed when correlating performance and connectivity measures (all $p$'s $> 0.11$). There were significant performance differences between younger and low performing older adults in 1-, 2-, and 3-back and between younger and high performing older adults in 2- and 3-back ($p$'s $< 0.05$). Comparing brain activity (mean parameter estimates from the univariate fMRI GLM) between high- and low-performing older adults did not show significant differences ($p$'s $> 0.48$).

Additional analyses such as BMS ranking of single models (Supplementary Table S2), results from BMA analyses

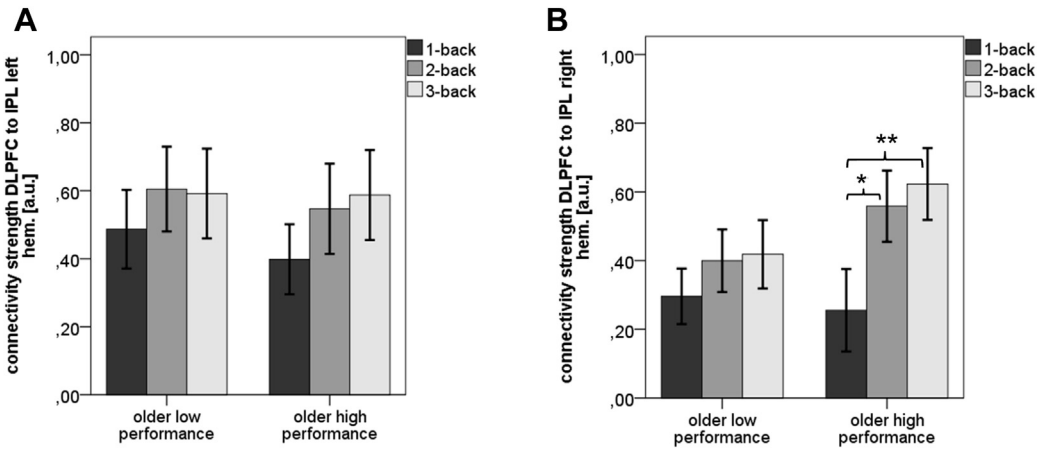


**Fig. 5.** Mean parameter estimates of effective connectivity ± standard error of the DLPFC to IPL connectivity in older adults with high versus low performance in the left (panel A) and right hemisphere (panel B). $^{*}p < 0.05$ and $^{**}p < 0.008$ (Bonferroni corrected for 6 planned comparisons).

(Supplementary Table S3), driving inputs (Supplementary Table S4), and intrinsic connectivity (Supplementary Table S5) are reported in the Supplementary Material.

## 4. Discussion

In keeping with previous research, age-related decrements in WM-performance observed in the present study were most pronounced at high levels of WM load. Neural activation in frontoparietal regions showed a WM load by age interaction, indicating both higher activations during 1-back and lower activations during 3-back in older compared to younger participants. On the level of effective connectivity, fMRI data of both age groups were best explained by a "backward" model, including WM-dependent connectivity from DLPFC to IPL in both hemispheres. Most importantly, WM load-dependent modulation of this connectivity was found to be reduced in older adults. Although WM load-dependent connectivity from DLPFC to IPL increased with increasing load in younger adults, this WM load-dependent increase was abolished in older adults in both hemispheres (Fig. 4, panels A and B).

### 4.1. N-back performance and fMRI GLM analyses

The findings of WM load-dependent decrements in WM-performance and alterations in frontoparietal activation patterns in older adults are in line with a previously published ROI-based analysis of a subsample of this study (Heinzel et al., 2014a) as well as other studies (Nagel et al., 2011; Nyberg et al., 2009; Schneider-Garces et al., 2010). As the magnitude of performance differences between age groups increased from 1- to 2-back but not from 2- to 3-back, this may imply that 2- and 3-back involve common subprocesses (e.g., updating) that are not at work during 1-back. Results from the GLM fMRI whole-brain analyses support the notion of lower neural efficiency and capacity (Barulli and Stern, 2013) as described in the CRUNCH model (Reuter-Lorenz and Cappell, 2008) and provide further evidence that age-related changes in WM-dependent frontoparietal brain activation may not simply be described as an "over- or underactivation" but rather in terms of a reduced adaptivity to increasing task demands.

### 4.2. Bayesian model selection

For the first time, these results offer an insight into complex age-related changes in WM-dependent and load-sensitive effective connectivity by means of DCM in conjunction with BMS. BMS family selection results suggested that WM-dependent network architecture itself was similar in younger and older adults in the left hemisphere ("backward" WM-dependent DLPFC to IPL connectivity). In the right hemisphere, the "backward" model family achieved the highest exceedance probability in both groups as well; however, the probabilities for the "forward" model family were also relatively high in younger adults. Furthermore, model rankings of single models as reported in the Supplementary Table S2 indicated that there was no clear advantage for a single model in right hemispheric connectivity models in younger adults. Since random-effects model comparison is by definition a relative procedure, this result does not imply that the tested models would fit the data of younger participants poorly. Thus, the result suggests that there is a larger between-subject variability in selected models within the younger sample compared to older adults. One interpretation is that this reflects the ability of younger adults to apply different successful strategies to solve numerical WM tasks such as visual imagery of number-pairs/-triplets versus phonological rehearsal, which may relate to different neuronal mechanisms (Morrison et al., 2016). Although this line of reasoning remains speculative so far, it could be targeted in future studies regarding the link between neuronal architecture and cognitive strategies.

### 4.3. WM-dependent effective connectivity within the frontoparietal network

Crucially, effective connectivity from DLPFC to IPL differed prominently as a function of WM load and age. Younger adults were characterized bilaterally by a substantial WM-dependent increase in effective connectivity from the DLPFC to IPL with increasing WM load. In line with our hypotheses, this WM load-dependent increase of DLPFC to IPL connectivity was not found in older adults. It seems that in contrast to younger participants, older adults show no elevated DLPFC control of IPL at high WM load (see Fig. 4, panel B). However, our hypothesis of increased DLPFC to IPL connectivity at low WM load in older adults was not confirmed in left hemisphere and only at trend level in the right hemisphere. Thus, age-related alterations in effective connectivity seem to be characterized mainly by an inability to increase DLPFC to IPL connectivity at high WM load.

Taken together, older adults seem to have a relatively load-insensitive connectivity pattern at this connection. These results also extend ideas of the CRUNCH model by providing an age-related alteration of WM-dependent and importantly also load-sensitive effective DLPFC to IPL connectivity as a potential neuronal mechanism of previously reported age-related fronto-parietal activation changes as well as performance decrements.

### 4.4. Deficient top-down control in aging

The finding of a bilateral shift from WM load-sensitive DLPFC to IPL connectivity toward a WM-dependent but load-insensitive DLPFC to IPL connectivity in older adults, may reflect an age-related deficit in flexibly adapting top-down control to external task demands (Gazzaley et al., 2005, 2008). This could then result in a deficient early selection of relevant and suppression of irrelevant information as it has been demonstrated in WM tasks designed to specifically test this (Gazzaley et al., 2005; Geerligs et al., 2012). It has been suggested that age-related changes in WM processing may be associated with a reduction of proactive cognitive control strategies in the face of high task demand (Dew et al., 2012; Paxton et al., 2008; Velanova et al., 2007). This notion resonates with our evidence from DCM, showing an age-related decline on the level of load-sensitive effective connectivity from DLPFC to IPL. This may correspond to a previously reported age-related deficit (Velanova et al., 2007) in proactively controlling information that should be gated into and maintained in IPL-associated WM storage (Chein and Fiez, 2010; Guerin and Miller, 2011). However, this notion needs to be investigated more specifically by future studies including tasks that allow for isolating specific subprocesses within WM.

Most importantly, our findings can render previous notions of age-related top-down control deficits more precisely and integrate them with ideas of the CRUNCH model. Instead of a generally reduced top-down control during WM task performance, aging seems to be related to a deficient WM load-dependent modulation of top-down control.

### 4.5. Effective connectivity and WM performance

Another important finding of the present study is that a WM load-sensitive DLPFC to IPL connectivity in the right hemisphere may explain differences in WM performance within the older adults. Therefore, it seems that this mechanism can at least partially be described as "successful" in the sense of Grady (2012) as we found a more "youth-like" pattern of WM load-dependent increase

in high performing compared to low performing older adults. These results indicate that age-related left-hemispheric alterations in WM load-dependent frontoparietal top-down control might in part be compensated by a relatively intact modulation in the right hemisphere in high performing older adults. Since these performance-related differences were not detected in the univariate fMRI GLM analysis, DCM parameter estimates might have been more sensitive to uncover subtle differences in neural processing.

### 4.6. Limitations

Since DCM analyses only allow a rather limited set of connections to be included into the tested model space, no conclusions about the contribution of connections between other regions involved in WM processing may be drawn from the current DCM analyses. Furthermore, several interpretations cannot be directly deducted from our results. The n-back task does not allow differentiation of different process components according to the temporal stage of processing and the specific WM component (e.g., updating vs. maintenance). Disentangling of different subprocesses in WM would require other tasks, such as the delayed match to sample (Sternberg) WM task. A larger sample of older adults was recruited to allow for comparing performance-related subgroups within the older group. Thus, findings of WM load-sensitive effective connectivity in younger adults require replication in larger sample size; but, it should be noted that the dominance of a WM-dependent DLPFC to IPL "backward" network architecture already replicates a previous study (Deserno et al., 2012).

### 4.7. Conclusion

Behavioral and fMRI GLM analyses replicate previous findings of WM performance decrements and a reduced adaptivity of frontoparietal neural activations to increasing WM load in older adults. Importantly, by means of DCM and BMS, we show that aging is associated with a reduction in WM load-dependent modulation of prefrontal to parietal "backward" connectivity. The degree of WM load-dependent adaptivity in right hemispheric DLPFC to IPL connectivity was related to WM performance in older adults and thus may reveal a neural mechanism underlying successful maintenance of WM functioning throughout the lifespan. The results of the present study advance our understanding of neuronal mechanisms that can be described in terms of deficient WM load-dependent modulation of top-down control in aging. Thus, the presented findings can integrate implications from theoretical models and previous neuroimaging studies of age-related alterations in brain functioning during WM.

## Disclosure statement

The authors have no actual or potential conflicts of interest.

## Acknowledgements

This work was supported by German National Academic Foundation scholarships to SH and RCL, the German Ministry for Education and Research (BMBF 01QG87164 and 01GS08195 and 01GQ0914), the German Research Foundation (Deutsche Forschungsgemeinschaft, DFG, FOR 1617: grant RA1047/2-1 and in part by the DFG SPP 1772: grants RA1047/4-1 and HE 7464/1-1), and by a MaxNetAging award to M.A.R. LD is supported by the Max Planck Society. Fractions of the current work are part of an unpublished thesis. The authors thank L. Oliveras Puig, W.-R. Brockhaus, and S. Saase for assistance during data acquisition and T. Wüstenberg for support during conventional fMRI analyses.

## Appendix. Supplementary data

Supplementary data associated with this article can be found, in the online version, at http://dx.doi.org/10.1016/j.neurobiolaging.2017.05.005.

## References

Ashburner, J., Friston, K.J., 2005. Unified segmentation. NeuroImage 26, 839–851.
Baddeley, A., 2003. Working memory: looking back and looking forward. Nat. Rev. Neurosci. 4, 829–839.
Barulli, D., Stern, Y., 2013. Efficiency, capacity, compensation, maintenance, plasticity: emerging concepts in cognitive reserve. Trends Cogn. Sci. 17, 502–509.
Bledowski, C., Kaiser, J., Rahm, B., 2010. Basic operations in working memory: Contributions from functional imaging studies. Behav. Brain Res. 214, 172–179.
Bledowski, C., Rahm, B., Rowe, J.B., 2009. What "works" in working memory? Separate systems for selection and updating of critical information. J. Neurosci. Off. J. Soc. Neurosci. 29, 13735–13741.
Cabeza, R., Daselaar, S.M., Dolcos, F., Prince, S.E., Budde, M., Nyberg, L., 2004. Task-independent and task-specific age effects on brain activity during working memory, visual attention and episodic retrieval. Cereb. Cortex 14, 364–375.
Chein, J.M., Fiez, J.A., 2010. Evaluating models of working memory through the effects of CONCURRENT irrelevant information. J. Exp. Psychol. Gen. 139, 117–137.
Christophel, T.B., Hebart, M.N., Haynes, J.-D., 2012. Decoding the Contents of visual short-term memory from human visual and parietal cortex. J. Neurosci. 32, 12983–12989.
Cohen, J.D., Perlstein, W.M., Braver, T.S., Nystrom, L.E., Noll, D.C., Jonides, J., Smith, E.E., 1997. Temporal dynamics of brain activation during a working memory task. Nature 386, 604–608.
Craik, F.I.M., Salthouse, T.A., 2011. The Handbook of Aging and Cognition, third ed. Psychology Press, New York, NY.
Curtis, C.E., D'Esposito, M., 2003. Persistent activity in the prefrontal cortex during working memory. Trends Cogn. Sci. 7, 415–423.
Deserno, L., Sterzer, P., Wüstenberg, T., Heinz, A., Schlagenhauf, F., 2012. Reduced prefrontal-parietal effective connectivity and working memory deficits in schizophrenia. J. Neurosci. Off. J. Soc. Neurosci. 32, 12–20.
Dew, I.T.Z., Buchler, N., Dobbins, I.G., Cabeza, R., 2012. Where is ELSA? The early to late shift in aging. Cereb. Cortex 22, 2542–2553.
Edin, F., Klingberg, T., Johansson, P., McNab, F., Tegnér, J., Compte, A., 2009. Mechanism for top-down control of working memory capacity. Proc. Natl. Acad. Sci. U. S. A. 106, 6802–6807.
Folstein, M.F., Folstein, S.E., McHugh, P.R., 1975. "Mini-mental state": a practical method for grading the cognitive state of patients for the clinician. J. Psychiatr. Res 12, 189–198.
Friston, K.J., Harrison, L., Penny, W., 2003. Dynamic causal modeling. NeuroImage 19, 1273–1302.
Friston, K.J., Mechelli, A., Turner, R., Price, C.J., 2000. Nonlinear responses in fMRI: the Balloon model, Volterra kernels, and other hemodynamics. NeuroImage 12, 466–477.
Gazzaley, A., Clapp, W., Kelley, J., McEvoy, K., Knight, R.T., D'Esposito, M., 2008. Age-related top-down suppression deficit in the early stages of cortical visual memory processing. Proc. Natl. Acad. Sci. U. S. A. 105, 13122–13126.
Gazzaley, A., Cooney, J.W., Rissman, J., D'Esposito, M., 2005. Top-down suppression deficit underlies working memory impairment in normal aging. Nat. Neurosci. 8, 1298–1300.
Gazzaley, A., D'Esposito, M., 2007. Top-down modulation and normal aging. Ann. N. Y. Acad. Sci. 1097, 67–83.
Gazzaley, A., Rissman, J., Cooney, J., Rutman, A., Seibert, T., Clapp, W., D'Esposito, M., 2007. Functional interactions between prefrontal and visual association cortex contribute to top-down modulation of visual processing. Cereb. Cortex 17 (Suppl 1), i125–i135.
Geerligs, L., Saliasi, E., Maurits, N.M., Lorist, M.M., 2012. Compensation through increased functional connectivity: neural correlates of Inhibition in old and young. J. Cogn. Neurosci. 24, 2057–2069.
Grady, C., 2012. The cognitive neuroscience of ageing. Nat. Rev. Neurosci. 13, 491–505.
Guerin, S.A., Miller, M.B., 2011. Parietal cortex tracks the amount of information retrieved even when it is not the basis of a memory decision. NeuroImage 55, 801–807.
Heinzel, S., Lorenz, R.C., Brockhaus, W.-R., Wüstenberg, T., Kathmann, N., Heinz, A., Rapp, M.A., 2014a. Working memory load-dependent brain response predicts behavioral training gains in older adults. J. Neurosci. 34, 1224–1233.
Heinzel, S., Lorenz, R.C., Pelz, P., Heinz, A., Walter, H., Kathmann, N., Rapp, M.A., Stelzel, C., 2016. Neural correlates of training and transfer effects in working memory in older adults. NeuroImage 134, 236–249.
Heinzel, S., Riemer, T.G., Schulte, S., Onken, J., Heinz, A., Rapp, M.A., 2014b. Catechol-O-methyltransferase (COMT) Genotype Affects age-related changes in plasticity in working memory: a Pilot study. Biomed. Res. Int. 2014, 414351.
Heinzel, S., Schulte, S., Onken, J., Duong, Q.-L., Riemer, T.G., Heinz, A., Kathmann, N., Rapp, M.A., 2014c. Working memory training improvements and gains in non-trained cognitive tasks in young and older adults. Neuropsychol. Dev. Cogn. B Aging Neuropsychol. Cogn. 21, 146–173.

Lancaster, J.L., Woldorff, M.G., Parsons, L.M., Liotti, M., Freitas, C.S., Rainey, L., Kochunov, P.V., Nickerson, D., Mikiten, S.A., Fox, P.T., 2000. Automated Talairach atlas labels for functional brain mapping. Hum. Brain Mapp. 10, 120–131.
Logan, J.M., Sanders, A.L., Snyder, A.Z., Morris, J.C., Buckner, R.L., 2002. Under-recruitment and Nonselective Recruitment: Dissociable neural mechanisms associated with aging. Neuron 33, 827–840.
Maldjian, J.A., Laurienti, P.J., Kraft, R.A., Burdette, J.H., 2003. An automated method for neuroanatomic and cytoarchitectonic atlas-based interrogation of fMRI data sets. NeuroImage 19, 1233–1239.
Matthäus, F., Schmidt, J.-P., Banerjee, A., Schulze, T.G., Demirakca, T., Diener, C., 2012. Effects of age on the structure of functional connectivity networks during episodic and working memory demand. Brain Connect 2, 113–124.
McNab, F., Klingberg, T., 2008. Prefrontal cortex and basal ganglia control access to working memory. Nat. Neurosci. 11, 103–107.
Montojo, C.A., Courtney, S.M., 2008. Differential neural activation for updating rule versus stimulus information in working memory. Neuron 59, 173–182.
Morrison, A.B., Rosenbaum, G.M., Fair, D., Chein, J.M., 2016. Variation in strategy use across measures of verbal working memory. Mem. Cognit. 44, 922–936.
Nagel, I.E., Preuschhof, C., Li, S.-C., Nyberg, L., Bäckman, L., Lindenberger, U., Heekeren, H.R., 2011. Load modulation of BOLD response and connectivity predicts working memory performance in younger and older adults. J. Cogn. Neurosci. 23, 2030–2045.
Nee, D.E., Brown, J.W., Askren, M.K., Berman, M.G., Demiralp, E., Krawitz, A., Jonides, J., 2013. A meta-analysis of executive components of working memory. Cereb. Cortex 23, 264–282.
Nyberg, L., Dahlin, E., Stigsdotter Neely, A., Bäckman, L., 2009. Neural correlates of variable working memory load across adult age and skill: dissociative patterns within the fronto-parietal network. Scand. J. Psychol. 50, 41–46.
Nyberg, L., Lövdén, M., Riklund, K., Lindenberger, U., Bäckman, L., 2012. Memory aging and brain maintenance. Trends Cogn. Sci. 16, 292–305.
Owen, A.M., McMillan, K.M., Laird, A.R., Bullmore, E., 2005. N-back working memory paradigm: a meta-analysis of normative functional neuroimaging studies. Hum. Brain Mapp. 25, 46–59.
Park, D.C., Reuter-Lorenz, P., 2009. The adaptive brain: aging and neurocognitive scaffolding. Annu. Rev. Psychol. 60, 173–196.
Paxton, J.L., Barch, D.M., Racine, C.A., Braver, T.S., 2008. Cognitive control, goal maintenance, and prefrontal function in healthy aging. Cereb. Cortex 18, 1010–1028.
Penny, W.D., Stephan, K.E., Daunizeau, J., Rosa, M.J., Friston, K.J., Schofield, T.M., Leff, A.P., 2010. Comparing families of dynamic causal models. PLoS Comput. Biol. 6, e1000709.
Rajah, M.N., D'Esposito, M., 2005. Region-specific changes in prefrontal function with age: a review of PET and fMRI studies on working and episodic memory. Brain J. Neurol. 128, 1964–1983.
Reuter-Lorenz, P.A., Cappell, K.A., 2008. Neurocognitive aging and the compensation hypothesis. Curr. Dir. Psychol. Sci. 17, 177–182.
Reuter-Lorenz, P.A., Jonides, J., Smith, E.E., Hartley, A., Miller, A., Marshuetz, C., Koeppe, R.A., 2000. Age differences in the frontal lateralization of verbal and spatial working memory revealed by PET. J. Cogn. Neurosci. 12, 174–187.
Reuter-Lorenz, P.A., Park, D.C., 2014. How does it STAC Up? Revisiting the scaffolding theory of aging and cognition. Neuropsychol. Rev. 24, 355–370.
Rottschy, C., Langner, R., Dogan, I., Reetz, K., Laird, A.R., Schulz, J.B., Fox, P.T., Eickhoff, S.B., 2012. Modeling neural correlates of working memory: a coordinate-based meta-analysis. NeuroImage 60, 830–846.
Schmidt, A., Smieskova, R., Aston, J., Simon, A., Allen, P., Fusar-Poli, P., McGuire, P.K., Riecher-Rössler, A., Stephan, K.E., Borgwardt, S., 2013. Brain connectivity abnormalities predating the onset of psychosis: correlation with the effect of medication. JAMA Psychiatry 70, 903–912.
Schmidt, K.-H., Metzler, P., 1992. Wortschatztest (WST). Beltz, Weinheim.
Schneider-Garces, N.J., Gordon, B.A., Brumback-Peltz, C.R., Shin, E., Lee, Y., Sutton, B.P., Maclin, E.L., Gratton, G., Fabiani, M., 2010. Span, CRUNCH, and beyond: working memory capacity and the aging brain. J. Cogn. Neurosci. 22, 655–669.
Steffener, J., Habeck, C.G., Stern, Y., 2012. Age-related changes in task related functional network connectivity. PLoS One 7, e44421.
Stephan, K.E., Penny, W.D., Daunizeau, J., Moran, R.J., Friston, K.J., 2009. Bayesian model selection for group studies. NeuroImage 46, 1004–1017.
Stern, Y., Habeck, C., Moeller, J., Scarmeas, N., Anderson, K.E., Hilton, H.J., Flynn, J., Sackeim, H., van Heertum, R., 2005. Brain networks associated with cognitive reserve in healthy young and old adults. Cereb. Cortex 15, 394–402.
Todd, J.J., Marois, R., 2004. Capacity limit of visual short-term memory in human posterior parietal cortex. Nature 428, 751–754.
Velanova, K., Lustig, C., Jacoby, L.L., Buckner, R.L., 2007. Evidence for frontally Mediated controlled processing differences in older adults. Cereb. Cortex 17, 1033–1046.
Verhaeghen, P., Cerella, J., 2002. Aging, executive control, and attention: a review of meta-analyses. Neurosci. Biobehav. Rev. 26, 849–857.
Wager, T.D., Smith, E.E., 2003. Neuroimaging studies of working memory: a meta-analysis. Cogn. Affect. Behav. Neurosci. 3, 255–274.